NATIONAL ADVISORY COMMITTEE FOR AERONAUTICS

TECHNICAL NOTE

No. 1668

INVESTIGATION OF EFFECTS OF GEOMETRIC DIHEDRAL ON LOW-SPEED STATIC STABILITY AND YAWING CHARACTERISTICS OF AN UNTAPERED 45° SWEPTBACK-WING MODEL OF ASPECT RATIO 2.61

By M. J. Queijo and Byron M. Jaquet

Langley Aeronautical Laboratory
Langley Field, Va.

Washington

September 1948

NATIONAL ADVISORY COMMITTEE FOR AERONAUTICS

TECHNICAL NOTE NO. 1668

INVESTIGATION OF EFFECTS OF GEOMETRIC DIHEDRAL ON LOW-SPEED STATIC STABILITY AND YAWING CHARACTERISTICS OF AN UNTAPERED 45° SWEPTBACK-WING MODEL OF ASPECT RATIO 2.61

By M. J. Queijo and Byron M. Jaquet

SUMMARY

An investigation was conducted to determine the effects of geometric dihedral on the low-speed static stability and yawing characteristics of an untapered 45° sweptback-wing model of aspect ratio 2.61. The results of the tests indicated that an increase in positive dihedral resulted in an increase in the rolling moment due to sideslip and also caused the maximum value of rolling moment due to sideslip to occur at increasingly higher lift coefficients. Increasing positive or negative dihedral caused a decrease in the lift-curve slope and an increase in the variation of lateral force with sideslip. Dihedral had no appreciable effect on the yawing moment due to sideslip.

The rolling moment due to yawing became more positive with increasingly positive dihedral and became less positive with increasingly negative dihedral. The rate of change of rolling moment due to yawing with dihedral angle was nearly independent of lift coefficient. The yawing moment due to yawing was nearly independent of lift coefficient for low and moderate lift coefficients and showed no definite trends at higher lift coefficients. The lateral force due to yawing became more positive with an increase in positive or negative dihedral and showed little variation with lift coefficient through the low and moderate range of lift coefficients. At higher lift coefficients, the lateral force due to yawing became more positive.

INTRODUCTION

Estimation of the dynamic flight characteristics of airplanes requires a knowledge of the component forces and moments resulting from the orientation of the airplane with respect to the air stream and from the angular velocity of the airplane about each of its three axes. The forces and moments resulting from the orientation of the airplane usually are expressed as the static stability derivatives, which are readily determined in conventional wind-tunnel tests. The forces and moments related to the angular motions (rotary derivatives) generally have been estimated from theory because of the lack of a convenient experimental technique.

The recent application of the rolling-flow and curved-flow principle of the Langley stability tunnel has made possible the determination of both the rotary and static stability derivatives with about the same ease. Unpublished data have indicated that although the rotary stability derivatives of unswept wings of moderate or high aspect ratio can be predicted quite accurately from the available theory, the use of sweep - and, perhaps, low aspect ratio - introduces effects which are not readily amenable to theoretical treatment. For this reason, a systematic research program has been established for the purpose of determining the effects of various geometric variables on both rotary and static stability characteristics.

The present investigation is concerned with the determination of the effects of geometric dihedral on the static stability and yawing characteristics of an untapered 45° swept wing of aspect ratio 2.61.

SYMBOLS

All forces and moments are given with respect to the stability axes with the origin at the quarter-chord point of the mean aerodynamic chord of the wing. The positive direction of the forces, moments, angular displacements, and velocities are shown in figure 1. The symbols and coefficients used herein are defined as follows:

C_L lift coefficient (L/qS)

$C_{L'}$ lift coefficient based on lift of one panel of wing with dihedral and on area of entire wing

C_Y lateral-force coefficient (Y/qS)

C_X longitudinal-force coefficient (X/qS)

C_l rolling-moment coefficient (L/qSb)

C_n yawing-moment coefficient (N/qSb)

C_m pitching-moment coefficient $(M/qS\bar{c})$

L lift, pounds

Y lateral force, pounds

X longitudinal force, pounds

L rolling moment about X-axis, foot-pounds

N yawing moment about Z-axis, foot-pounds

M pitching moment about Y-axis, foot-pounds

q	dynamic pressure, pounds per square foot $\left(\frac{1}{2}\rho V_o^2\right)$
ρ	mass density of air, slugs per cubic foot
V_o	free-stream velocity, feet per second
V	local velocity, feet per second
S	wing area (zero dihedral wing), square feet
b	span of wing, measured perpendicular to plane of symmetry (zero dihedral wing), feet
c	chord of wing, measured parallel to plane of symmetry, feet
y	absolute value of spanwise distance from plane of symmetry to any station on wing quarter-chord line
$\bar{c}$	mean aerodynamic chord, feet $\left(\frac{2}{S}\int_0^{b/2} c^2\,dy\right)$
$\bar{x}$	rearward distance from coordinate origin (airplane center of gravity) to aerodynamic center
$\bar{y}$	effective lateral center-of-pressure location of the resultant load caused by rolling
A	aspect ratio (b^2/S)
α	angle of attack measured in a vertical plane parallel to the plane of symmetry, degrees
ψ	angle of yaw (equal to $-\beta$), degrees
β	angle of sideslip, degrees, unless otherwise indicated
Λ	angle of sweep, positive for sweepback, degrees
Γ	dihedral angle, degrees (unless otherwise specified)
$rb/2V_o$	yawing-velocity parameter
r	angular velocity in yaw, radians per second
R	radius of curvature of flight path
a_o	section lift-curve slope, per radian

$$C_{L_\alpha} = \frac{\partial C_L}{\partial \alpha}$$

$$C_{l_\psi} = \frac{\partial C_l}{\partial \psi}$$

$$C_{n_\psi} = \frac{\partial C_n}{\partial \psi}$$

$$C_{Y_\psi} = \frac{\partial C_Y}{\partial \psi}$$

$$C_{l_r} = \frac{\partial C_l}{\partial \frac{rb}{2V_o}}$$

$$C_{n_r} = \frac{\partial C_n}{\partial \frac{rb}{2V_o}}$$

$$C_{Y_r} = \frac{\partial C_Y}{\partial \frac{rb}{2V_o}}$$

$\partial C_{l_\psi}/\partial \Gamma$ dihedral-effectiveness parameter; rate of change of C_{l_ψ} with dihedral angle

$\partial C_{l_r}/\partial \Gamma$ rate of change of C_{l_r} with dihedral angle

Subscripts:

i induced

L left-wing panel

R right-wing panel

APPARATUS AND TESTS

The tests of the present investigation were made in the 6- by 6-foot test section of the Langley stability tunnel, in which curved flow can be simulated by curving the air stream about a stationary model.

The model tested was an untapered 45° sweptback wing (see fig. 2) with a 10-inch chord and NACA 0012 airfoil sections in planes normal to the leading edge. The model was constructed of laminated mahogany and consisted of two panels which were joined together by metal brackets. The brackets were made to give the model dihedral angles of 10°, 0°, -10°, and -20°. The model was rigidly attached to a single strut into which was built a strain-gage balance system by which all the forces and moments on the model were measured. A photograph of the model mounted on the support strut in the curved-flow test section is shown as figure 3. Some clearance was provided between the strut and the model. No attempt was made to seal the clearance gap because previous tests of a similar model showed that sealing the gap had negligible effect on the characteristics of the model.

Two series of tests were made. The first series consisted of straight-flow tests for each model configuration. The tests were made through a yaw-angle range from -30° to 30° for several angles of attack. The second series of tests were made in simulated yawing flight for each model configuration (Γ= 10°, 0°, -10°, and -20°). The yawing-flow tests were made at zero yaw angle and at stream curvatures corresponding to values of $rb/2V_o$ of 0, -0.031, -0.067, and -0.088, based on the span of the zero-dihedral model. Each model configuration was tested from about zero lift up to the stall.

All tests were made at a dynamic pressure of 24.9 pounds per square foot, which corresponds to a Mach number of 0.13 and a Reynolds number, based on the model mean aerodynamic chord, of 1.1×10^6.

CORRECTIONS

Approximate corrections for jet-boundary effect were applied to the angle of attack and to the longitudinal-force coefficient. A correction was also applied to the lateral force to account for the error caused by the static-pressure gradient across the curved-flow test section. The corrections used are:

$$\Delta C_X = -\delta_w \frac{S}{S'} C_L^2$$

$$\Delta\alpha = 57.3\delta_w \frac{S}{S'} C_L$$

$$\Delta C_Y = 4.0 \frac{v}{bS} \frac{rb}{2V}$$

where

δ_w boundary correction factor from reference 1

S' tunnel cross-section area at test section, feet

v volume of model, cubic feet

No corrections were made for tunnel blocking or support strut tares except for the derivatives C_{l_r}. In this case, the tare at zero lift coefficient was applied throughout the lift-coefficient range.

RESULTS AND DISCUSSION

Presentation of Data

All the test data are based on the area, span, and mean aerodynamic chord of the zero-dihedral model configuration. The data obtained from the straight-flow tests are presented in figures 4 and 5. Curves of lift coefficient C_L, longitudinal-force coefficient C_X, and pitching-moment coefficient C_m plotted against angle of attack for each model configuration ($\psi = 0^\circ$) are presented in figure 4. Curves of rolling-moment coefficient C_l, yawing-moment coefficient C_n, and lateral-force coefficient C_Y plotted against angle of yaw for several angles of attack and for each model configuration are shown in figure 5. The data obtained from the yawing-flow tests are presented in figure 6 as plots of C_l, C_n, and C_Y against $rb/2V_o$ for several angles of attack for each model configuration.

The variations of C_{l_ψ}, C_{n_ψ}, and C_{Y_ψ} with lift coefficient are shown in figure 7 for each model configuration in straight flow. The variations of C_{l_r}, C_{n_r}, and C_{Y_r} with lift coefficient are shown in figure 8 for each model configuration.

The effects of dihedral on the static longitudinal stability characteristics C_{L_α} and dC_m/dC_L are shown in figure 9. The effect of dihedral on the rolling-moment derivatives C_{l_ψ} and C_{l_r} for several lift coefficients is shown in figure 10. The variations of the parameters $\partial C_{l_\psi}/\partial\Gamma$ and $\partial C_{l_r}/\partial\Gamma$ with lift coefficient are shown in figure 11.

Straight-Flow Results

Lift characteristics.- The slopes of the lift curves at zero lift of figure 4 are presented as a function of dihedral angle in figure 9. The curve of figure 9 indicates that the lift-curve slope decreases with increasing positive or negative dihedral. The analysis of reference 2

shows that the variation of lift-curve slope with dihedral can be expressed as

$$\left(C_{L_\alpha}\right)_\Gamma = \left(C_{L_\alpha}\right)_{\Gamma=0^\circ} \cos^2 \Gamma \qquad (1)$$

where $\left(C_{L_\alpha}\right)_{\Gamma=0^\circ}$ is the lift-curve slope of the zero-dihedral model and $\left(C_{L_\alpha}\right)_\Gamma$ is the lift-curve slope of the same model with dihedral. The curve of $\left(C_{L_\alpha}\right)_\Gamma$ obtained by means of equation (1) and the measured value of $\left(C_{L_\alpha}\right)_{\Gamma=0^\circ}$ are presented in figure 9 for comparison with the experimentally obtained variation. The two curves generally are in good agreement and are consistent with similar results in reference 3.

Pitching-moment characteristics.- The pitching-moment data of figure 4 indicate that as the dihedral angle is made positive, the pitching moment generally becomes less positive. The slopes of the pitching-moment curves of figure 4 were measured at zero lift and are plotted in figure 9 as a curve of $\partial C_m/\partial C_L$ against dihedral angle. The slope $\partial C_m/\partial C_L$ generally becomes slightly less positive as the dihedral angle is made more positive.

Longitudinal-force characteristics.- The longitudinal force is nearly independent of dihedral angle for angles of attack up to about 12°. (See fig. 4.) At higher angles of attack the longitudinal-force coefficient generally decreases with either positive or negative dihedral.

Rolling-moment characteristics.- The rolling-moment data of figure 7 indicate that, for the wing tested, positive dihedral resulted in a positive displacement of the curve of C_{l_ψ} and negative dihedral resulted in a negative displacement of the curve of C_{l_ψ} at all lift coefficients. As the dihedral angle becomes more positive, the maximum value of C_{l_ψ} occurs at increasingly higher lift coefficients; whereas, increasing the dihedral negatively causes the maximum value of C_{l_ψ} to occur at increasingly lower lift coefficients. This trend is exactly the opposite to that reported in reference 3. The disagreement is believed to be caused by the differences in taper ratio and in camber of the two models. The model of reference 3 had a taper ratio 0.5 and a Rhode St. Genese 33 airfoil section.

The rolling-moment data of figure 7 were cross-plotted in figure 10 to give curves of C_{l_ψ} as a function of dihedral angle for several lift coefficients. The curves of figure 10 indicate that the slope of the curve of C_{l_ψ} against dihedral angle generally is constant in the -10° to 10° dihedral-angle range and decreases slightly in the -10° to -20° range. The same trend was indicated in reference 3. The slopes of the

curves of C_{l_ψ} of figure 10 were measured in the -10° to 10° dihedral-angle range and were plotted against lift coefficient in figure 11. The plot indicates that $\partial C_{l_\psi}/\partial\Gamma$ is nearly independent of lift coefficient up to a lift coefficient of about 0.5 and has a value of about 0.00011. At higher lift coefficients $\partial C_{l_\psi}/\partial\Gamma$ increases to 0.00017.

The curve of $\partial C_{l_\psi}/\partial\Gamma$ of reference 3 is included in figure 11 for comparison with the results of the present investigation. It is seen that the curves of the two investigations are quite different both in magnitude and in mode of variation with lift coefficient. In an attempt to explain these differences, an equation based on the methods of reference 4 and extended to include dihedral angle effects was derived. (See appendix.) The equation is

$$\frac{\partial C_{l_\psi}}{\partial\Gamma} = \frac{(A + 4)\cos\Lambda}{A + 4\cos\Lambda}\left(\frac{\partial C_{l_\psi}}{\partial\Gamma}\right)_{\Lambda=0} \tag{2}$$

where $\left(\frac{\partial C_{l_\psi}}{\partial\Gamma}\right)_{\Lambda=0°}$ is the dihedral effectiveness parameter of an unswept wing with the same aspect ratio as the wing under consideration and is obtained directly from figure 12 for aspect ratios from 1 to 16 and taper ratios of 1.0 and 0.5. Equation (2) gives a result of $\frac{\partial C_{l_\psi}}{\partial\Gamma} = 0.00013$ for the wing of the present investigation and a result of 0.000143 for the wing of reference 3. Although these calculated results are not very good checks on the experimental data, they do show that equation (2) gives the proper trends as far as magnitude is concerned. Little more may be said for the validity of equation (2) until more data are available for comparison with calculated results.

Yawing-moment characteristics.- The yawing-moment data of figure 7 indicate that C_{n_ψ} is nearly independent of dihedral for lift coefficients up to approximately $C_L = 0.5$. At higher lift coefficients the curves of C_{n_ψ} are irregular, but in general, C_{n_ψ} becomes more positive with increasingly negative dihedral and more negative with increasingly positive dihedral.

Lateral-force characteristics.- The lateral force due to yaw C_{Y_ψ} becomes more positive as the dihedral is made more positive or more negative. C_{Y_ψ} is nearly independent of lift coefficient up to about $C_L = 0.5$ and becomes irregular at higher lift coefficients. (See fig. 7.)

Yawing Flow

Rolling-moment characteristics.- The rolling-moment data of figure 8 indicate that the rolling moment due to yawing becomes more positive with increase in positive dihedral. Reference 5 indicates that the dynamic stability of an airplane decreases with a decrease in positive C_{l_r}. This result indicates that the use of negative dihedral might decrease the dynamic stability; however, whether negative dihedral is detrimental or beneficial to dynamic stability depends on the effect of dihedral angle on all the derivatives which affect dynamic stability. Figure 8 also indicates that C_{l_r} generally increases with lift coefficient over the low-lift-coefficient range.

The rolling-moment data of figure 8 were plotted in figure 10 as curves of C_{l_r} against dihedral for several lift coefficients. The derivative C_{l_r} varies approximately linearly with dihedral for a given lift coefficient. The slopes of the curves of figure 10 were measured and plotted in figure 11 as a curve of $\partial C_{l_r}/\partial\Gamma$ against lift coefficient. The parameter $\partial C_{l_r}/\partial\Gamma$ is practically independent of lift coefficient and has an average value of about 0.0040. The methods of reference 4 were extended to include the effects of small amounts of dihedral, and the following equation was derived (see appendix) for a sweptback wing with dihedral:

$$\frac{\partial C_{l_r}}{\partial\Gamma} = \frac{1}{12}\frac{\pi A \sin\Lambda}{A + 4\cos\Lambda} \tag{3}$$

where Γ is in radians. For the wing used in this investigation, equation (3) gives a value $\frac{\partial C_{l_r}}{\partial\Gamma} = 0.0890$ and converting Γ to degrees gives a value $\frac{\partial C_{l_r}}{\partial\Gamma} = 0.0016$. This value is less than half of the average value (0.0040) obtained in the tests reported herein. Although equation (3) indicates the proper trends of the effect of sweep on the parameter $\partial C_{l_r}/\partial\Gamma$, the magnitude of the effect is much too low. It is possible that the value $\partial C_{l_r}/\partial\Gamma$ given by equation (3) should be considered simply as an increment due to sweep and that it should be added to the value of $\partial C_{l_r}/\partial\Gamma$ of unswept wings in order to get the total value for a swept wing. (Such was found to be the case in reference 4 for the derivative C_{l_β} of swept wings.) Whether this hypothesis is correct cannot be determined at this time because of the lack of data on the derivative $\partial C_{l_r}/\partial\Gamma$ of unswept and swept wings.

Yawing-moment characteristics.- The yawing-moment data of figure 8 indicate that C_{n_r} is nearly independent of dihedral and also of

lift coefficient up to a lift coefficient of about $C_L = 0.5$. The curves are irregular at higher lift coefficients.

Lateral-force characteristics.- The lateral-force data of figure 8 indicate that increasing the positive or negative dihedral generally makes C_{Y_r} less negative and that C_{Y_r} varies only slightly with lift coefficient.

CONCLUSIONS

An investigation was conducted in the 6- by 6-foot test section of the Langley stability tunnel to determine the effects of dihedral on the aerodynamic characteristics of an untapered 45° sweptback-wing model of aspect ratio 2.61 in straight flow and in yawing flow. The results of the investigation have led to the following conclusions:

1. The results obtained for the low-speed static stability characteristics were generally consistent with those of previous investigations.

An increase in positive dihedral resulted in an increase in the rolling moment due to sideslip for all lift coefficients and also caused the maximum value of rolling moment due to sideslip to occur at increasingly higher lift coefficients.

Increasing positive or negative dihedral caused a decrease in the lift-curve slope and an increase in the variation of lateral force with sideslip.

Dihedral had no appreciable effect on the yawing moment due to sideslip.

2. The rolling moment due to yawing became more positive with increasingly positive dihedral and became less positive with increasingly negative dihedral.

3. The rate of change of rolling moment due to yawing with dihedral angle was practically independent of lift coefficient and had a value of about 0.0040 per degree of dihedral.

4. The yawing moment due to yawing was nearly independent of dihedral angle and lift coefficient for lift coefficients up to about 0.5 but showed no definite trend at higher lift coefficients.

5. The lateral force due to yawing became more positive with increase in positive or negative dihedral and showed little variation with lift coefficient.

Langley Aeronautical Laboratory
National Advisory Committee for Aeronautics
Langley Field, Va., April 14, 1948

APPENDIX

THEORETICAL DERIVATION OF $\partial C_{l_\beta}/\partial\Gamma$ AND $\partial C_{l_r}/\partial\Gamma$

Approximate equations were derived in reference 4 for the stability derivatives of swept wings without dihedral. The methods of reference 4 are extended herein to evaluate the parameters $\partial C_{l_\beta}/\partial\Gamma$ and $\partial C_{l_r}/\partial\Gamma$.

Dihedral Effectiveness Parameter

For wings with dihedral the change in angle of attack, resulting from sideslip, can be shown to be $\Delta\alpha = \beta \sin \Gamma$, where $\Delta\alpha$ is measured in planes perpendicular to each wing panel and parallel to the relative wind. For an antisymmetrical load distribution the induced angle in the same planes is approximately $\Delta\alpha_i = \frac{4C_L'}{\pi A}$. The lift-curve slope of an infinite skewed wing is $a_o \cos \Lambda$; therefore, from lifting-line theory

$$C_L' = \frac{1}{2}(\Delta\alpha - \Delta\alpha_i)a_o \cos \Lambda \tag{A1}$$

Substitution of the values of $\Delta\alpha$ and $\Delta\alpha_i$ into equation (A1) gives

$$C_L' = \frac{1}{2}\left(\beta \sin \Gamma - \frac{4C_L'}{\pi A}\right)a_o \cos \Lambda$$

or

$$C_L' = \frac{1}{2} \frac{Aa_o \cos \Lambda}{A + \frac{2a_o \cos \Lambda}{\pi}} \beta \sin \Gamma$$

If 2π is substituted in the denominator for a_o, then

$$C_L' = \frac{1}{2} \frac{Aa_o \cos \Lambda}{A + 4 \cos \Lambda} \beta \sin \Gamma \tag{A2}$$

The coefficient C_L' is of the same magnitude but of opposite sign for the two wing panels. The rolling-moment coefficient for the entire wing therefore is given by

$$C_l = -2C_L'\frac{\bar{y}}{b} \tag{A3}$$

Substitution of the value of C_L' given by equation (A2) into equation (A3) results in

$$C_l = -\frac{Aa_o \cos \Lambda}{A + 4 \cos \Lambda} \beta \sin \Gamma \frac{\bar{y}}{b}$$

If Γ is small, then $\sin \Gamma = \Gamma$, and

$$\frac{C_{l_\beta}}{\Gamma} = -\frac{1}{2} \frac{Aa_o \cos \Lambda}{A + 4 \cos \Lambda} \frac{\bar{y}}{b/2} \tag{A4}$$

where Γ is in radians. For unswept wings, equation (A4) gives

$$\left(\frac{C_{l_\beta}}{\Gamma}\right)_{\Lambda=0^\circ} = -\frac{1}{2} \frac{Aa_o}{A + 4} \frac{\bar{y}}{b/2} \tag{A5}$$

If the approximation is made that sweep has no effect on $\bar{y}$, then equations (A4) and (A5) may be combined to give the following equation:

$$\frac{C_{l_\beta}}{\Gamma} = \frac{(A + 4) \cos \Lambda}{A + 4 \cos \Lambda}\left(\frac{C_{l_\beta}}{\Gamma}\right)_{\Lambda=0^\circ} \tag{A6}$$

The values of $\left(\frac{C_{l_\beta}}{\Gamma}\right)_{\Lambda=0^\circ}$ given in figure 16 of reference 6 for aspect ratios 6 to 16 and taper ratios 1.0 and 0.5 have been extrapolated to low aspect ratios by the procedure used in reference 4. The extrapolated curves are presented in figure 12.

Rate of Change of Rolling Moment Due to

Yawing with Dihedral

A swept wing with dihedral undergoes a change in angle of attack in flight in a curved path. The change in angle of attack can be shown to be given approximately by

$$\Delta\alpha = \frac{\left(y - \frac{b}{4}\right)\tan \Lambda + \bar{x}}{R} \sin \Gamma \tag{A7}$$

The velocity over any section of the left wing panel is

$$V_L = r(R + y) \tag{A8}$$

and, for the right wing panel

$$V_R = r(R - y) \tag{A9}$$

The part of the wing loading caused by the flight-path curvature is unsymmetrical because of the velocity gradient across the wing span; therefore, the rate of change of lift on any section with angle of attack is given approximately by

$$\frac{Aa_o \cos \Lambda}{A + 4 \cos \Lambda}\left(\frac{V}{V_o}\right)^2$$

The rolling moment for rectangular wings is

$$C_l = \frac{1}{b^2}\int_0^{b/2}\left(C_{L'_L} - C_{L'_R}\right)y \, dy$$

or

$$C_l = \frac{Aa_o \cos \Lambda}{A + 4 \cos \Lambda} \frac{1}{b^2} \int_0^{b/2} \left[\left(\frac{V_L}{\bar{V}_o} \right)^2 + \left(\frac{V_R}{\bar{V}_o} \right)^2 \right] \Delta\alpha_y \, dy \tag{A10}$$

By means of equations (A8), (A9), and (A10) and if Γ is assumed to be small, it can be shown that

$$\frac{C_{l_r}}{\Gamma} = \frac{1}{4} \frac{Aa_o \cos \Lambda}{A + 4 \cos \Lambda} \left(\frac{1}{6} \tan \Lambda + \frac{\bar{x}}{b/2} \right)$$

If $\bar{x}$ is zero (as in the tests reported herein) and 2π is substituted for a_o, then

$$\frac{C_{l_r}}{\Gamma} = \frac{1}{12} \frac{\pi A \sin \Lambda}{A + 4 \cos \Lambda} \tag{A11}$$

REFERENCES

1. Silverstein, Abe, and White, James A.: Wind-Tunnel Interference with Particular Reference to Off-Center Positions of the Wing and to the Downwash at the Tail. NACA Rep. No. 547, 1935.

2. Purser, Paul E., and Campbell, John P.: Experimental Verification of a Simplified Vee-Tail Theory and Analysis of Available Data on Complete Models with Vee Tails. NACA Rep. No. 823, 1945.

3. Maggin, Bernard, and Shanks, Robert E.: The Effect of Geometric Dihedral on the Aerodynamic Characteristics of a 40° Swept-Back Wing of Aspect Ratio 3. NACA TN No. 1169, 1946.

4. Toll, Thomas A., and Queijo, M. J.: Approximate Relations and Charts for Low-Speed Stability Derivatives of Swept Wings. NACA TN No. 1581, 1948.

5. Sternfield, Leonard: Some Considerations of the Lateral Stability of High-Speed Aircraft. NACA TN No. 1282, 1947.

6. Pearson, Henry A., and Jones, Robert T.: Theoretical Stability and Control Characteristics of Wings with Various Amounts of Taper and Twist. NACA Rep. No. 635, 1938.

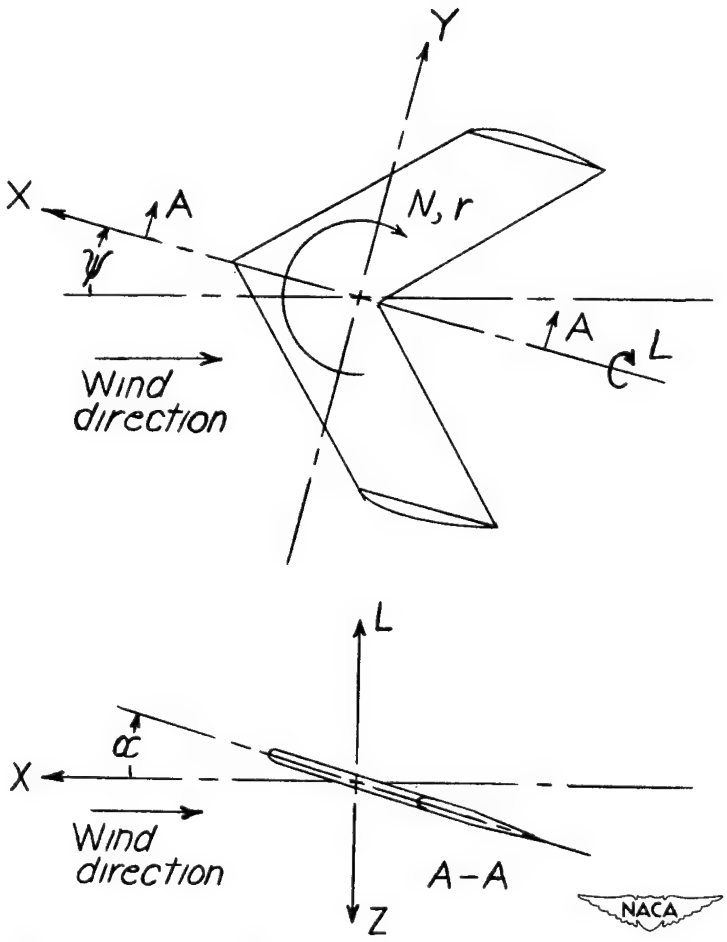

Figure 1.- The stability system of axes. Arrows indicate positive directions of forces, moments, angular velocities, and angular displacements.

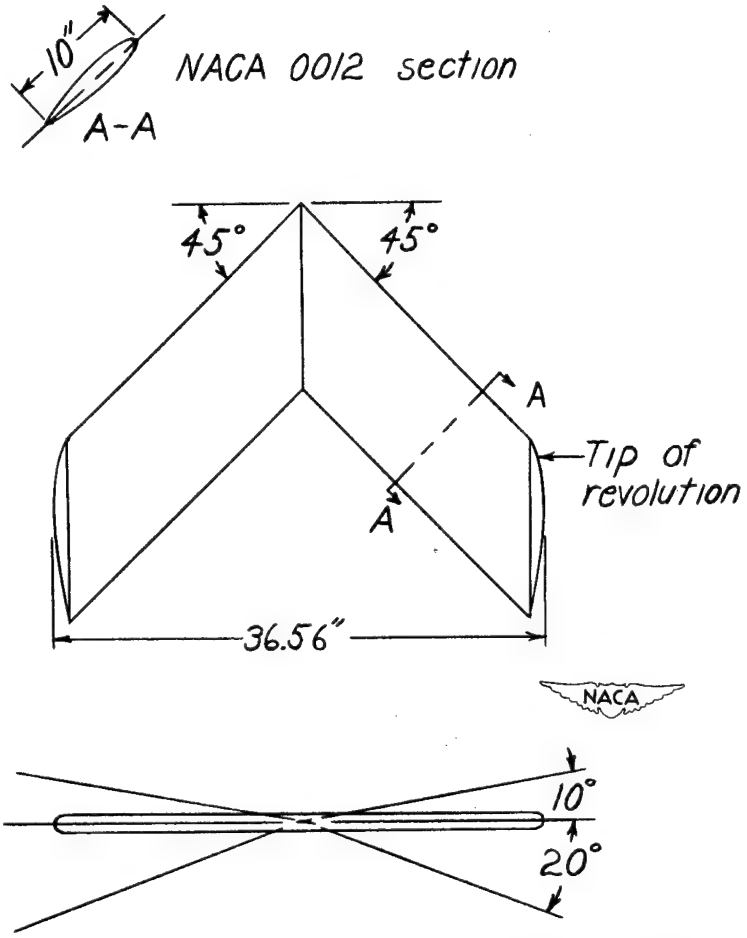

Figure 2.- Diagram of model tested.

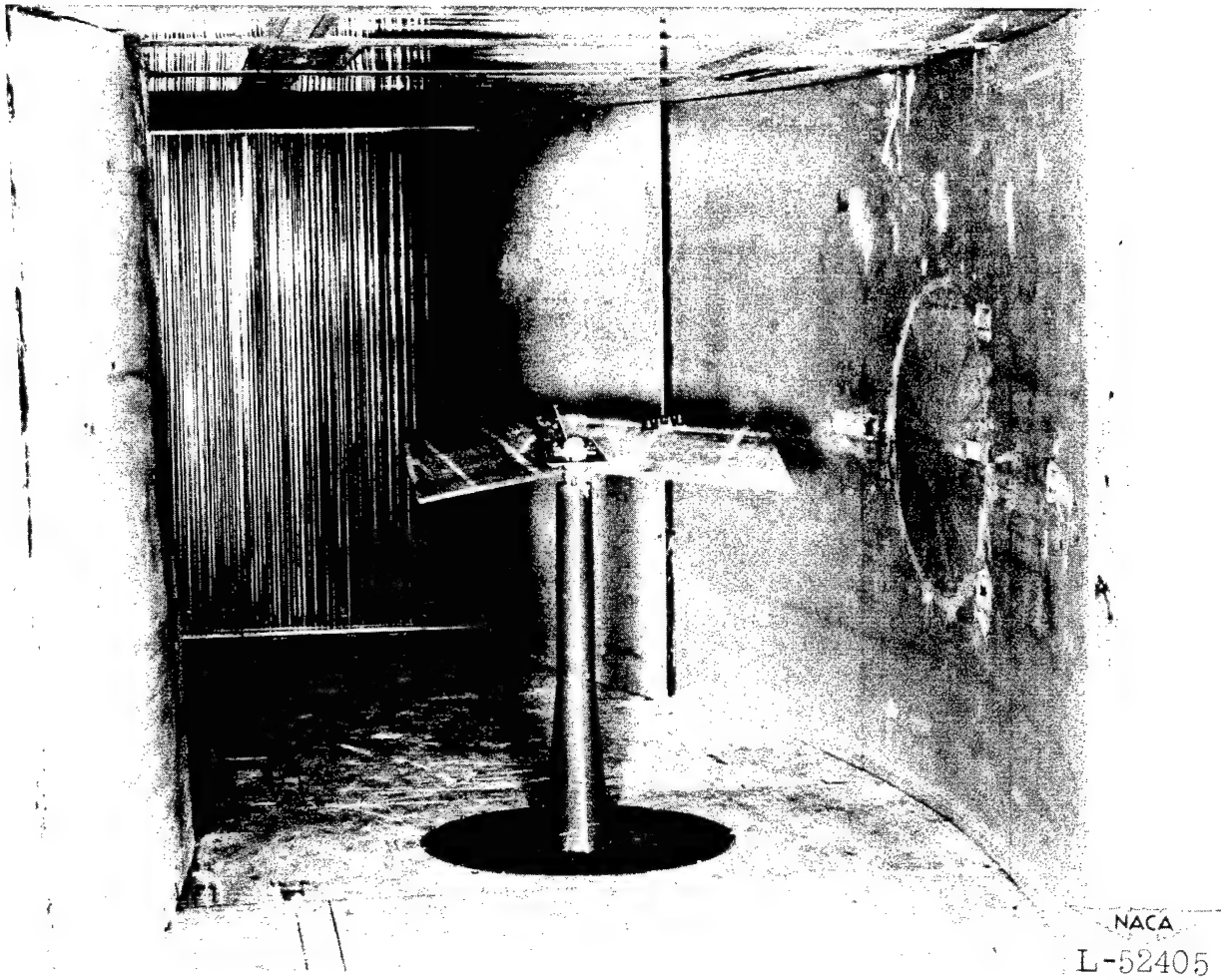

Figure 3.- Rear view of untapered 45° sweptback-wing model in the 6- by 6-foot curved-flow test section of the Langley stability tunnel. $\alpha = 10^{\circ}$; $\Gamma = 10^{\circ}$.

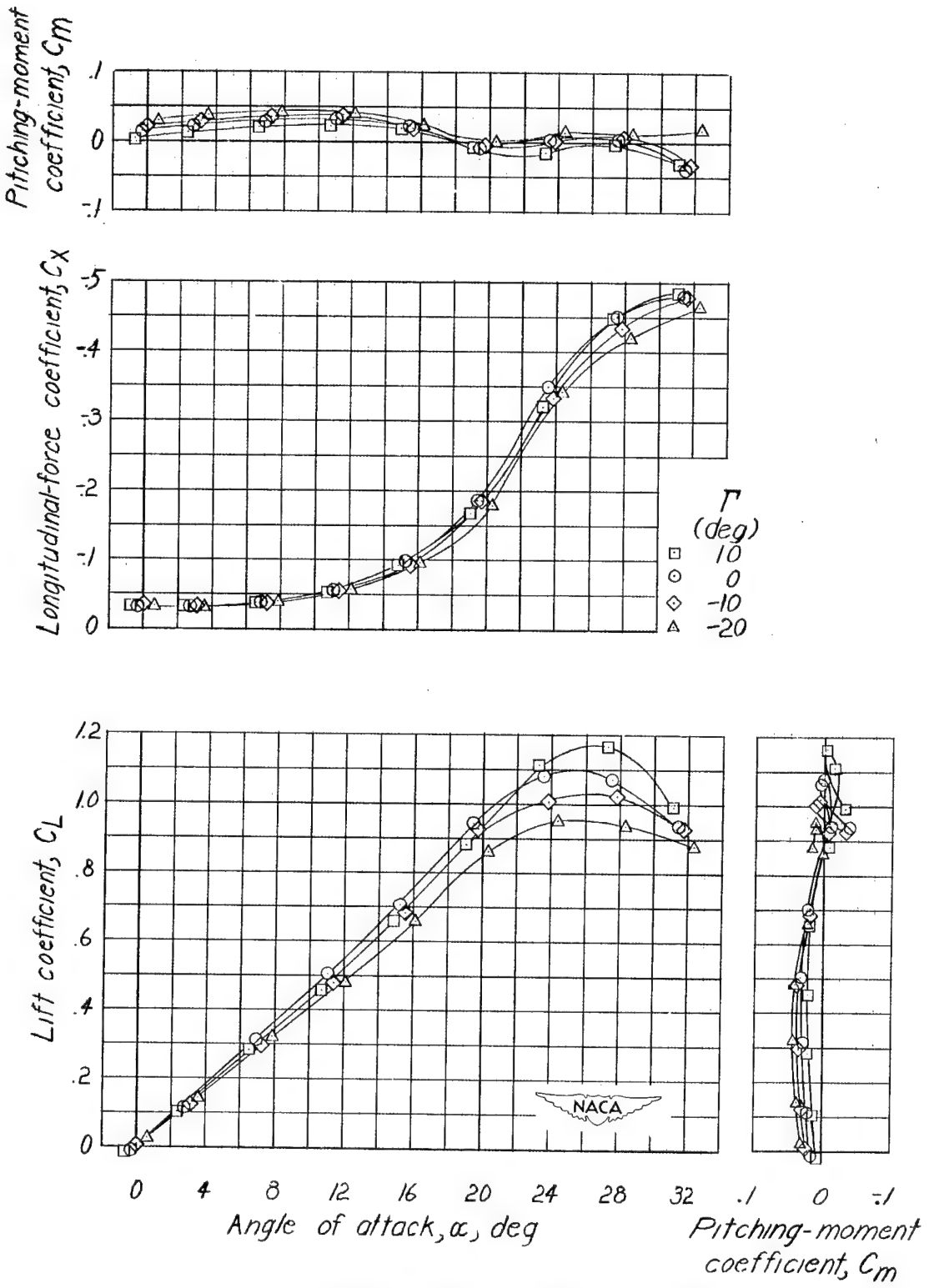

Figure 4.-Basic longitudinal-stability data of a 45° sweptback wing of aspect ratio 2.61 in straight flow. $\psi = 0°$.

Figure 5.- Basic lateral-stability data of a 45° sweptback wing of aspect ratio 2.61 in straight flow.

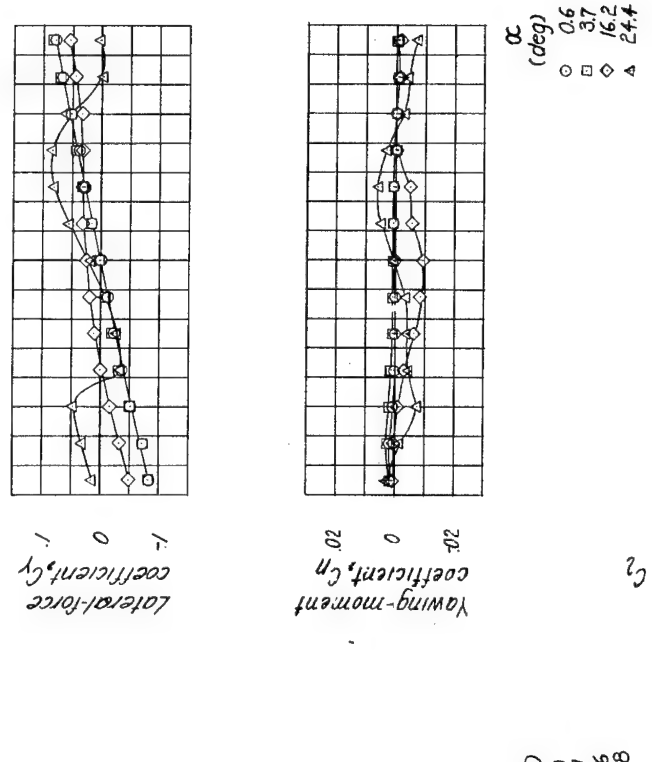

(d) $\Gamma = -20°$

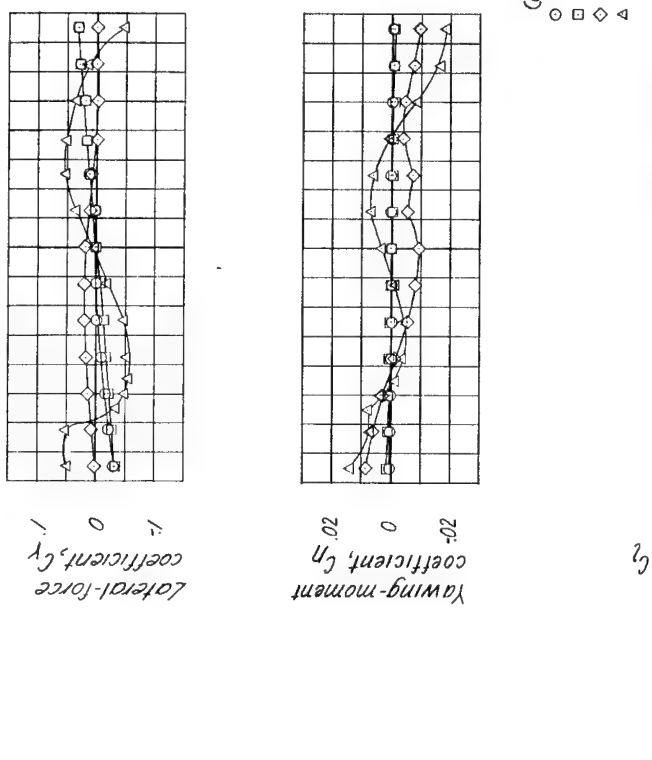

(c) $\Gamma = -10°$

Figure 5 - Concluded.

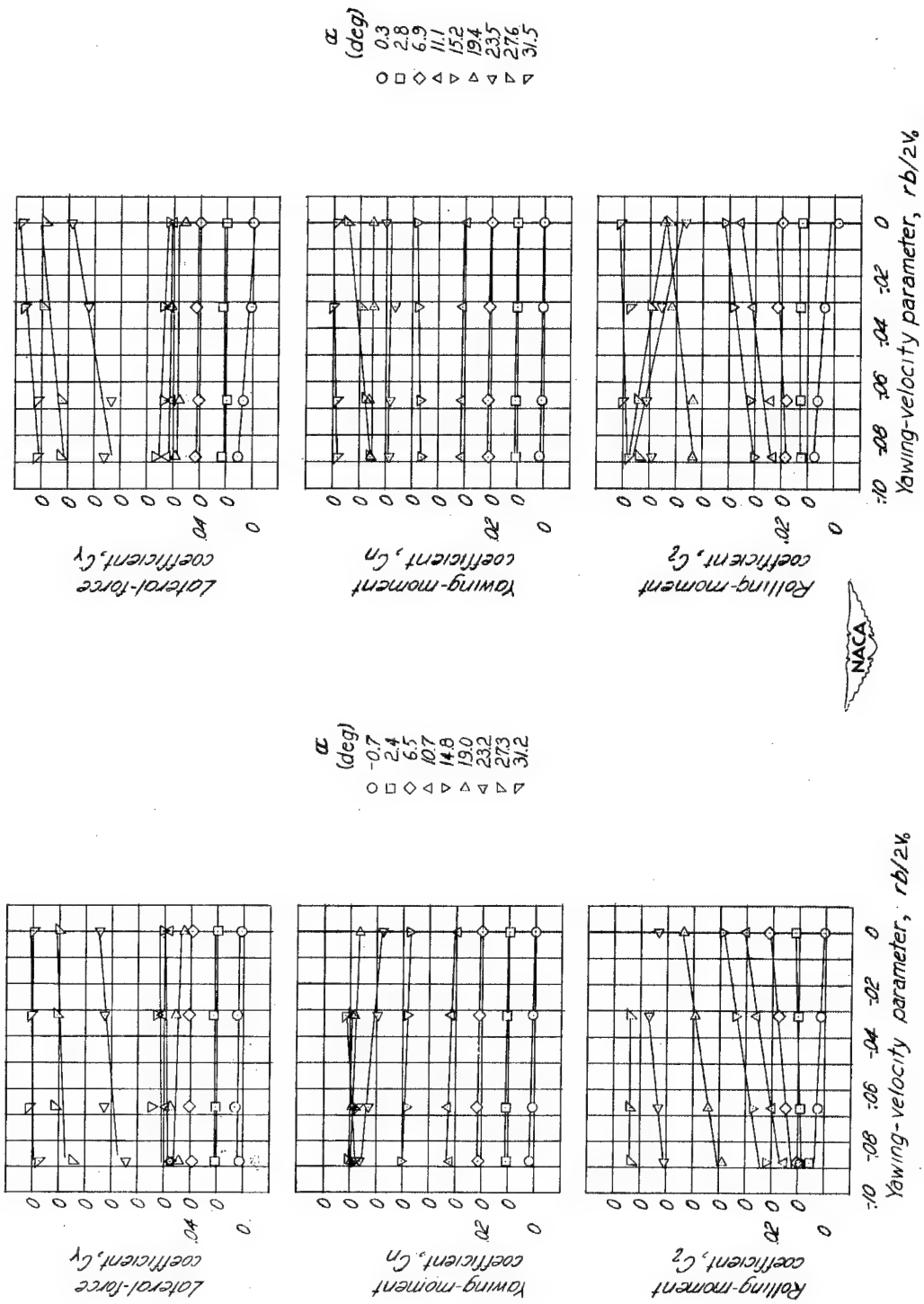

Figure 6.- Basic lateral-stability data of a 45° sweptback wing of aspect ratio 2.61 in yawing flow.

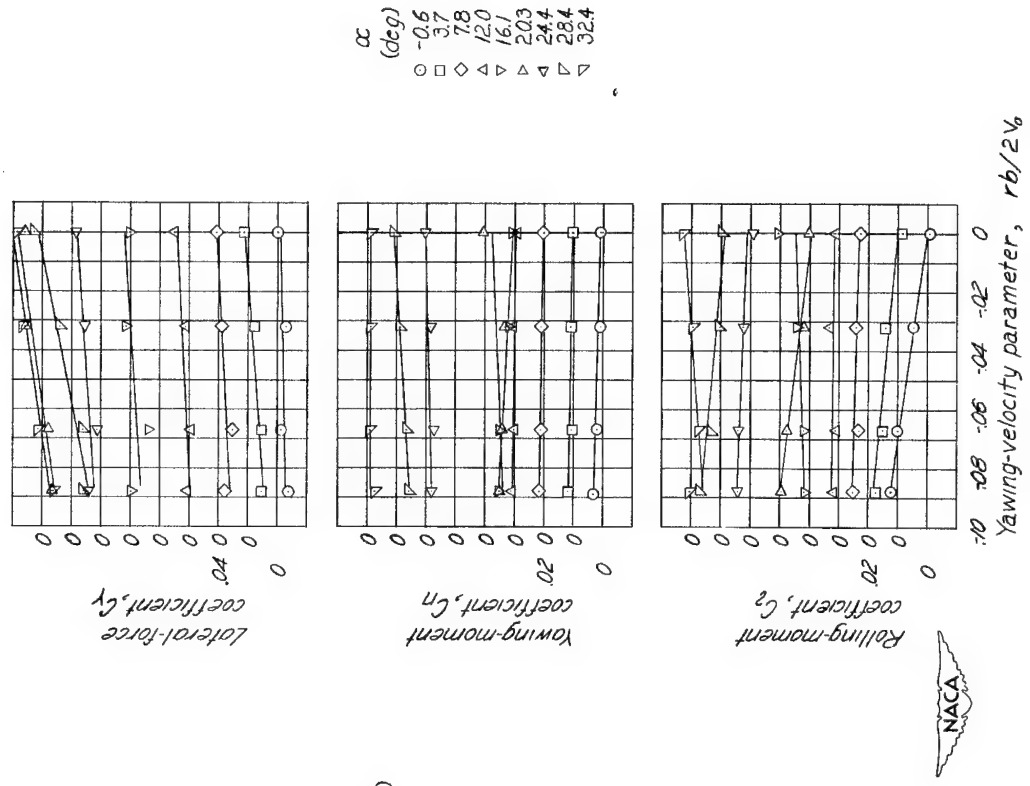

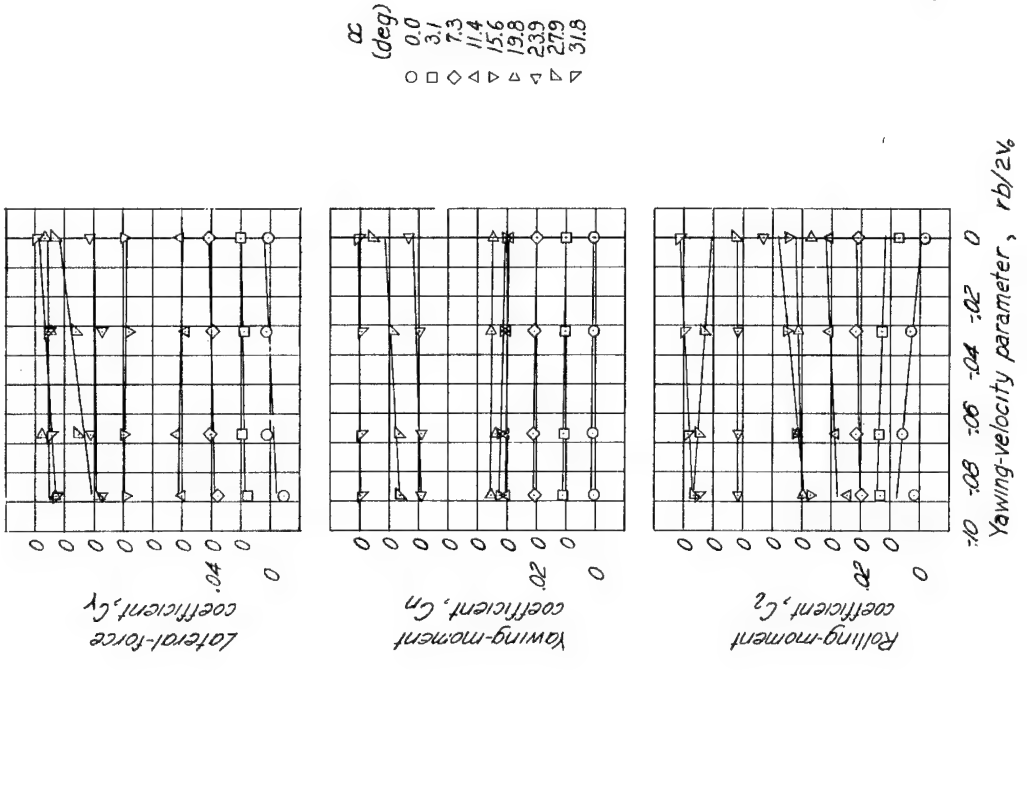

Figure 6.- Concluded.

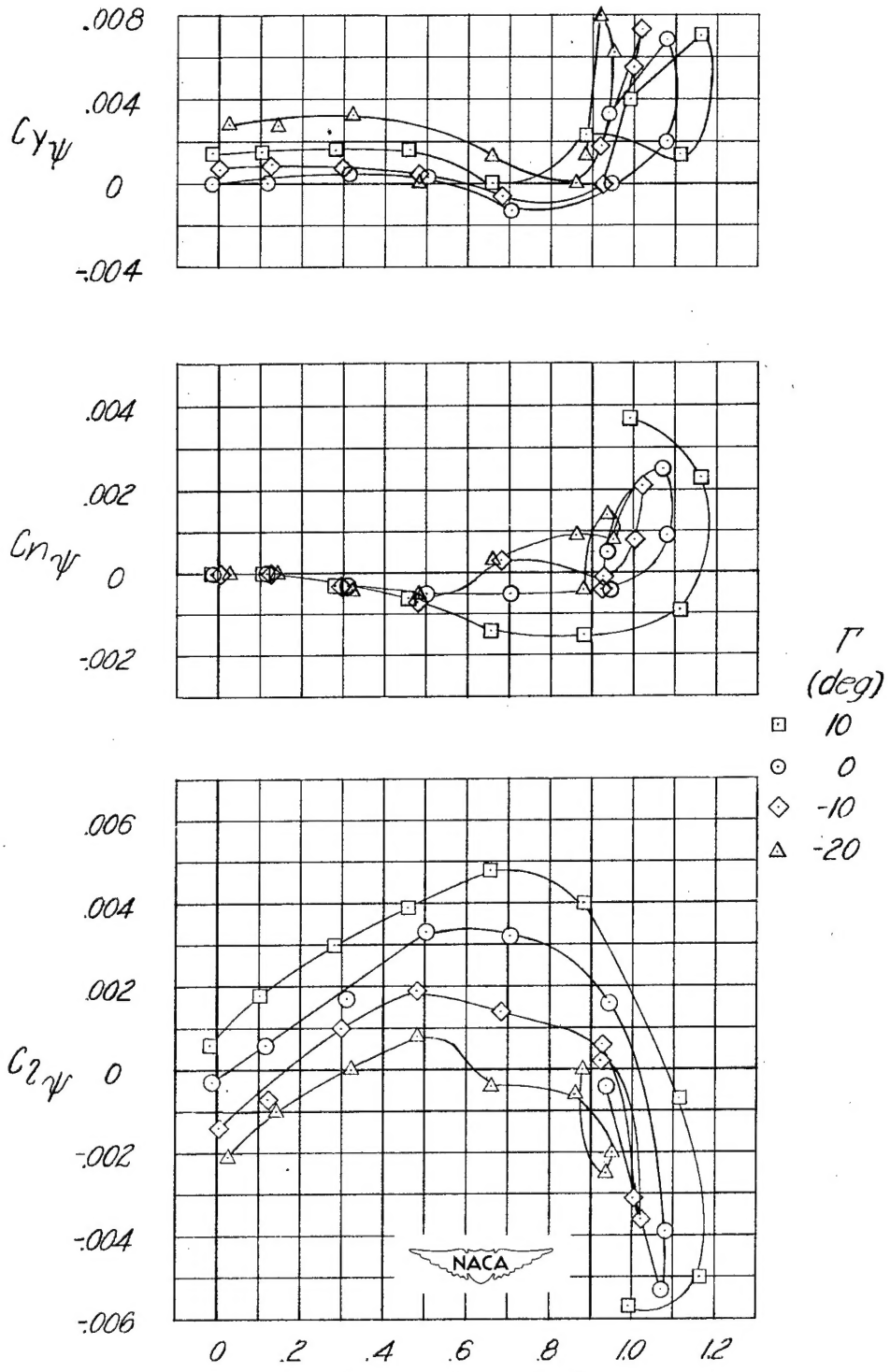

Figure 7.- Effect of dihedral angle on the variation of C_{l_ψ}, C_{n_ψ}, and C_{y_ψ} with lift coefficient for a 45° sweptback wing of aspect ratio 2.61.

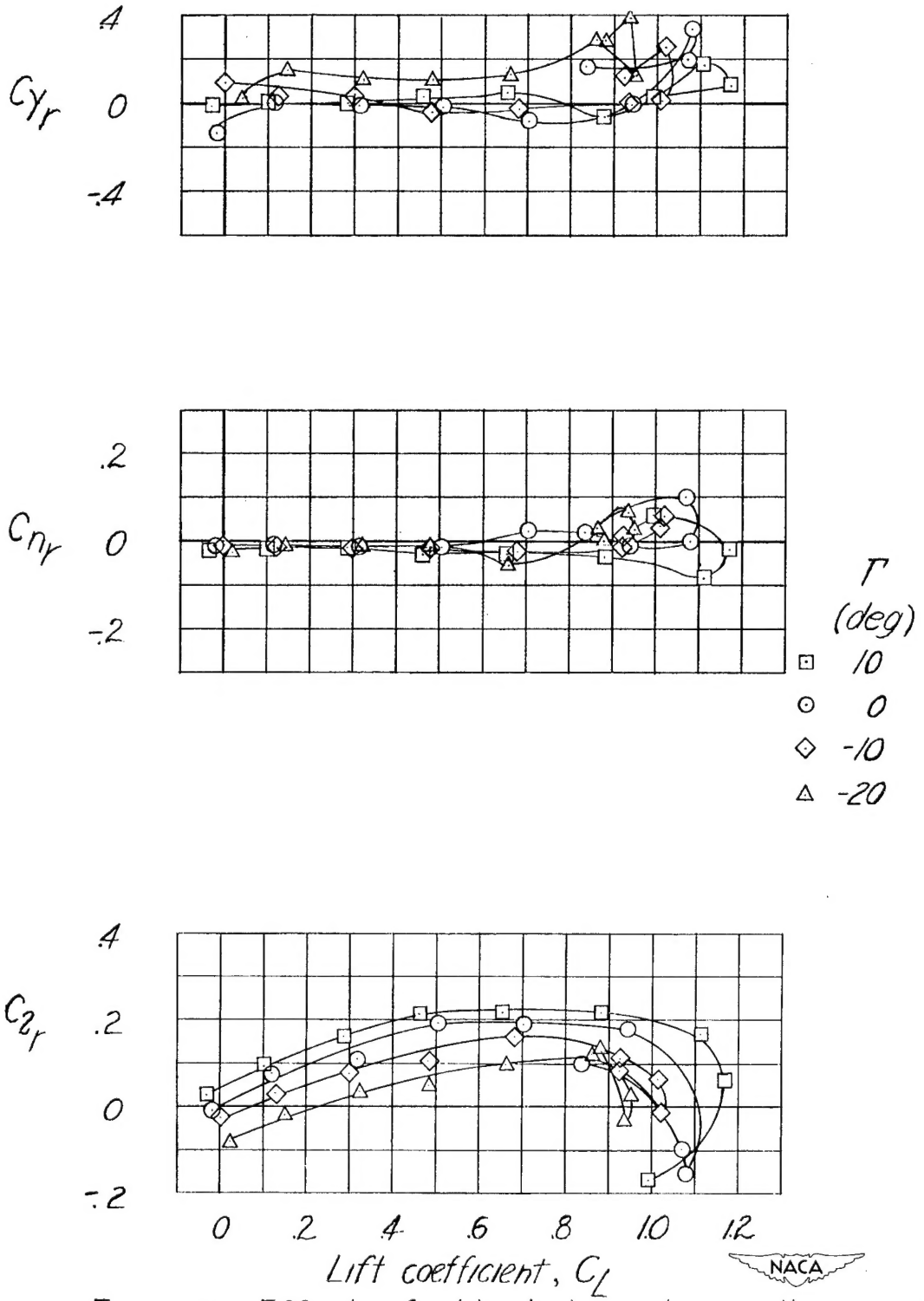

Figure 8.- Effect of dihedral angle on the variation of C_{l_r}, C_{n_r}, and C_{Y_r} with lift coefficient for a 45° sweptback wing of aspect ratio 2.61.

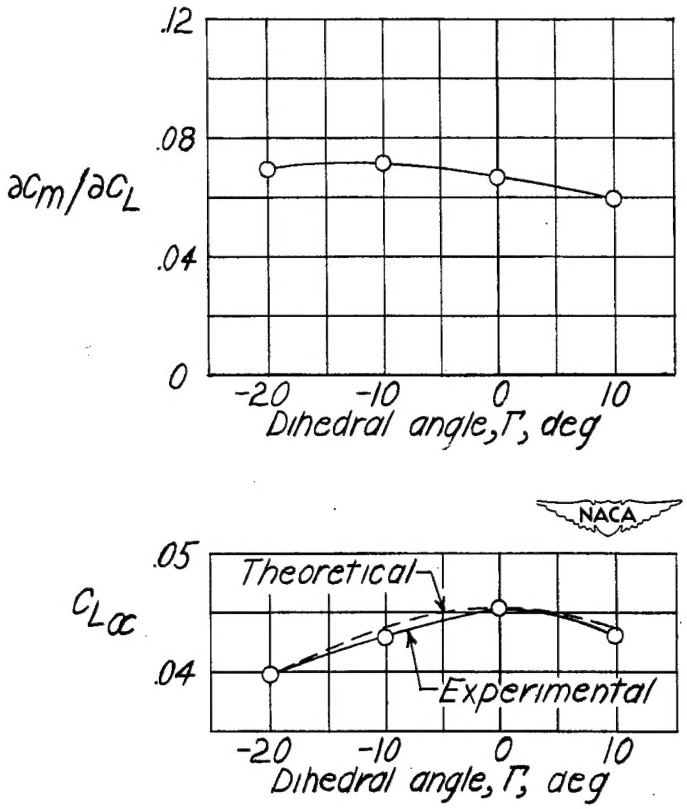

Figure 9.- Variation of $C_{L\alpha}$ and $\partial C_m/\partial \alpha$ with dihedral angle for a 45° swept-back wing. A=2.61; C_L=0.

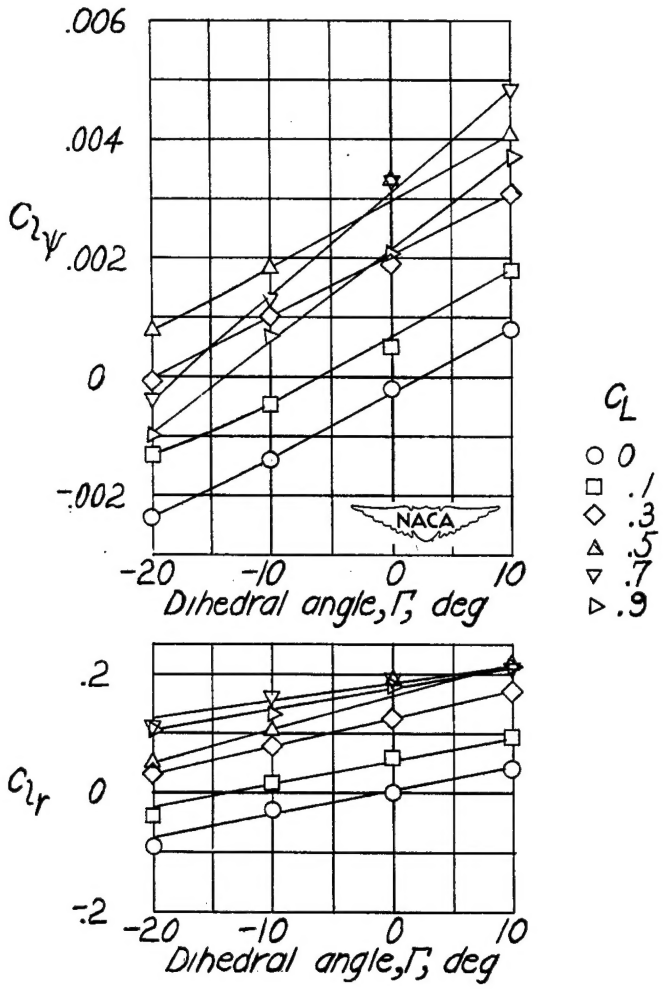

Figure 10.- Variation of C_{l_ψ} and C_{l_r} with dihedral angle.

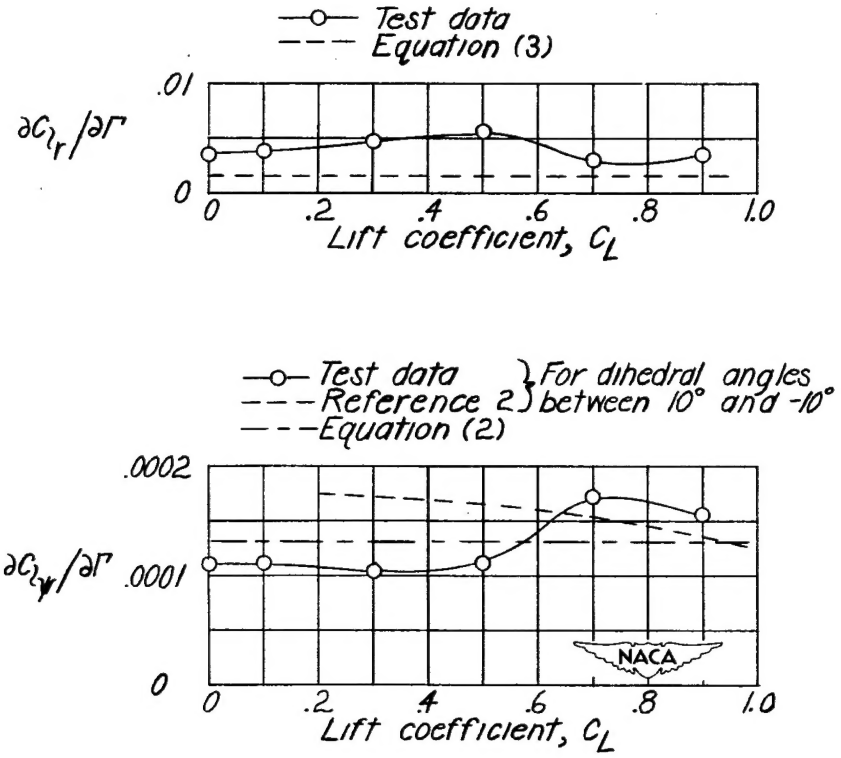

Figure 11.- Variation of $\frac{\partial C_{l_v}}{\partial \Gamma}$ and $\frac{\partial C_{l_r}}{\partial \Gamma}$ with lift coefficient for a 45° swept-back wing of aspect ratio 2.61.

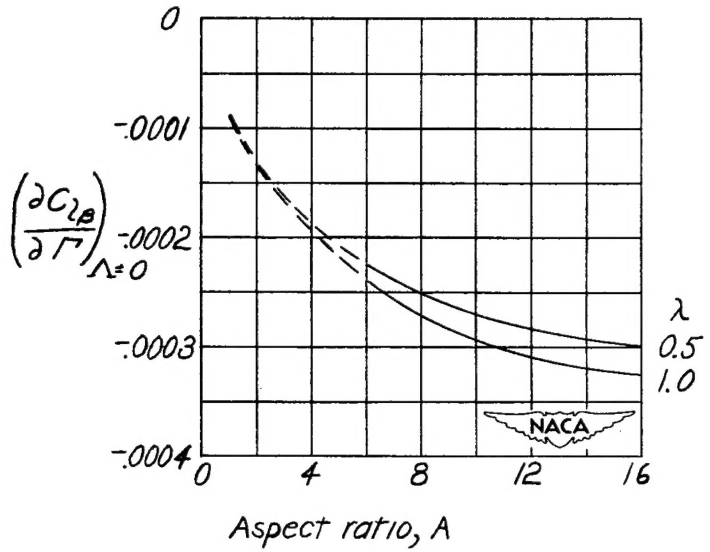

Figure 12.- Chart showing approximate values of the static dihedral-effectiveness parameter $\frac{\partial C_{l_\beta}}{\partial \Gamma}$ for unswept wings. $a_o = 5.67$.